Soft Matter

PAPER

View Article Online
View Journal | View Issue

Cite this: *Soft Matter*, 2016, 12, 5959

The effects of monovalent metal ions on the conformation of human telomere DNA using analytical ultracentrifugation†

Yating Gao, Sha Wu and Xiaodong Ye*

Received 1st May 2016,
Accepted 10th June 2016

DOI: 10.1039/c6sm01010e

www.rsc.org/softmatter

A human telomere DNA segment (HT-DNA) can fold into a G-quadruplex in the presence of some monovalent cations. These cations can interact with the phosphate groups of the DNA segment and/or with the O6 oxygen atom of guanines, which are called non-specific interactions and specific interactions, respectively. However, until now how these two interactions affect the structure of HT-DNA has not been well understood. In this study, a combination of analytical ultracentrifugation (AUC) and circular dichroism (CD) was used to explore the effects of these two interactions on the structure of a 22-mer single-stranded DNA with a sequence of 5′-AGGG(TTAGGG)$_3$-3′. The results showed that the standard sedimentation coefficient ($s_{20,w}$) of HT-DNA starts to increase when the concentration of potassium ions (C_{K^+}) is higher than 10.0 μM due to the formation of a G-quadruplex through specific interactions. Whereas, for a control DNA, a higher C_{K^+} value of 1.0 mM was needed for increasing $s_{20,w}$ due to non-specific interactions. Moreover, potassium ions could promote the formation of the G-quadruplex much more easily than lithium, sodium and cesium ions, presumably due to its appropriate size in the dehydrated state and easier dehydration. The molar mass of DNA at different cation concentrations was nearly a constant and close to the theoretical value of the molar mass of monomeric HT-DNA, indicating that what we observed is the structural change of individual DNA chains.

Introduction

Guanine-rich nucleic acids can fold into secondary structures called G-quadruplexes, four stranded DNA structures formed by stacked G-tetrad planes connected by eight Hoogsteen hydrogen bonds.[1–11] Human telomeres containing tandem repeats of sequence d(TTAGGG) at their extreme 3′-end are the complexes of DNA and proteins located at the ends of the chromosome, which play important roles in protecting chromosomes from fusion and degradation.[12–16] Under near-physiological conditions *in vitro*, telomere DNA sequences can fold into G-quadruplexes, which have shown abilities to interfere with cell function and may have a relationship with cell cancerization.[17,18] Until now, numerous methods have been used to analyze the structure of the human telomeric G-quadruplex *in vitro*, such as high-resolution solution state NMR,[5,8–10,19] single crystal diffraction,[20] molecular dynamics (MD) simulations,[21–23] circular dichroism (CD),[7,22,24–26] fluorescence,[7,27] differential scanning calorimetry (DSC),[28,29] mass spectrometry,[30,31] photon correlation spectroscopy,[32] atomic force microscopy (AFM),[33–35] analytical ultracentrifugation (AUC)[7,36–39] and so on.

The structure and stability of the human telomeric G-quadruplex are determined by the concentration[24] and sequence[9,21] of DNA and the nature and concentration of cations in solutions,[7–9,25,40,41] ligands[26,42] and cosolvents.[10,30] Among these conditions, cations play an important role. For example, HT-DNA can fold into an anti-parallel G-quadruplex structure in the presence of sodium ions while it forms a hybrid G-quadruplex in potassium ion solutions.[4,8,9] The increase in the concentration of cations can lead to an increase in the stability of the G-quadruplex as revealed by DSC and CD melting curves.[28,32] In order to understand the effect of cations on the G-quadruplex in detail, two interactions should be considered separately, the specific interactions and non-specific interactions. The specific interactions referring to the interactions between the G-quadruplex and cations in the center of a G-quartet or coordinated between two G-quartets are strongly related to the hydration extent and the size of the cations,[2,43] which are analogous to those found in host–guest systems such as the crown ethers.[44] These inner cations are all dehydrated ions and can stabilize the negative electrostatic potential created by the guanine O6 oxygen atoms within the quadruplex core.[22,45]

Hefei National Laboratory for Physical Sciences at the Microscale, Department of Chemical Physics, University of Science and Technology of China, Hefei, Anhui 230026, China. E-mail: xdye@ustc.edu.cn

† Electronic supplementary information (ESI) available. See DOI: 10.1039/c6sm01010e

Besides the specific interactions, owing to the polyelectrolyte nature of HT-DNA, it is surrounded by a cloud of counterions, which make up the non-specific interactions with HT-DNA. The non-specific interactions should also have an influence on the structure of the G-quadruplex.[25] However, until now only a few results about the effects of these two different interactions between cations and G-quadruplexes on the structure of guanine-rich telomere DNA have been reported. For example, using a fluorescent indicator to study the linkage between the K^+ binding and folding of HT-DNA with a sequence of 5′-AGGG TTAGGGTTAGGGTTAGGG-3′, Chaires *et al.* found that three K^+ ions bind to each HT-DNA chain when the concentration of free K^+ ions is 5 mM and the number increases to 8–10 when the potassium ions concentration is 20 mM.[46] Nevertheless, they also mentioned that this method cannot distinguish specific and non-specific binding from each other.

Analytical ultracentrifugation (AUC) is a powerful method to study the structural and hydrodynamic properties of nucleic acids.[7,36–39,47–53] In a centrifugation field with a suitable rotation velocity, the instrument records the sedimentation and diffusion processes of nucleic acids. The standard sedimentation coefficient ($s_{20,w}$), hydrodynamic radius (R_h) and weight-average molecular weight (M_w) can be determined. Thus, AUC can be used to characterize the influence of cations on the conformational change of nucleic acids. In an interesting precedent, Le *et al.* showed that the sedimentation coefficient of two G-quadruplex-forming sequences increases with the K^+ ions.[54] They mentioned that the low sedimentation coefficients at a low potassium concentration (25 mM) can be attributed to hydrodynamic non-ideality.[54] Thus, it is difficult to distinguish the contribution of a shift from a non-ideal solution to an ideal solution and from specific and non-specific potassium binding.[54] In this study, with a combination of AUC and CD, we investigated the effects of different salts on the conformation of a human telomeric DNA sequence 5′-AGGG(TTAGGG)$_3$-3′ (HT-DNA) with 10.0 mM tris(hydroxymethyl) aminomethane(Tris) to decrease the non-ideality. Due to the specific interactions, HT-DNA starts to fold from a random coil to a G-quadruplex structure when the concentration of potassium ions (C_{K^+}) is larger than 10.0 μM. When C_{K^+} reaches 1.0 mM, the folding of HT-DNA is complete and the non-specific interactions start to work. Furthermore, the effects of lithium, sodium and cesium ions on the formation of quadruplex structures of HT-DNA were also studied. The results show that K^+ can promote the formation of the G-quadruplex much more easily, presumably due to its appropriate size and easy dehydration.

Experimental section

Preparation of DNA aqueous solutions

A 22-mer HT-DNA and a control DNA with sequences of 5′-AGGGTTAGGGTTAGGGTTAGGG-3′ and 5′-TTATCTATGCTG TTACTCTGACTC-3′ were synthesized and purified using high performance liquid chromatography (HPLC) by Sangon Biological Engineering Technology and Services (Shanghai, China). The most important criterion for choosing the control DNA is that the control DNA cannot form a secondary structure in our study. Oligonucleotides were used as received and dissolved in 10.0 mM tris(hydroxymethyl)aminomethane (Tris)–HCl buffer solution (pH = 7.5) to give a stock solution with a concentration of ~50 μM. The DNA stock solution was heated to 95 °C for 5 min, and then slowly cooled down to room temperature. The stock solution was stored at −20 °C for future use. The concentrations of DNA were determined at 260 nm using a UV-vis spectrophotometer (UV-2802PCS, UNICO, Shanghai) with appropriate molar extinction coefficients at 260 nm (228.5 mM^{-1} cm^{-1} for HT-DNA, and 216.1 mM^{-1} cm^{-1} for control DNA, the values are calculated at http://biophysics.idtdna.com/UVSpectrum.html). Ultra-pure Milli-Q water with a resistivity of 18.2 MΩ cm used in all experiments was purified by filtration through a Millipore Gradient system after distillation. Tris(hydroxymethyl) aminomethane (Tris) (99%), concentrated hydrochloric acid (37.5%), lithium chloride (LiCl, 99%), sodium chloride (NaCl, 99%), potassium chloride (KCl, 99%) and cesium chloride (CsCl, 99%) from Sinopharm were used as received. The DNA solutions for sedimentation velocity and circular dichroism experiments were diluted from the DNA stock solution by 10.0 mM Tris–HCl buffer solutions with appropriate concentrations of salts (LiCl, NaCl, KCl or CsCl).

Circular dichroism (CD)

CD spectra were recorded on a JASCO J-810 spectrometer using a 1 mm path length quartz cuvette. The final concentration of the oligonucleotide was 8.0 μM in 10.0 mM Tris–HCl buffer solution (pH = 7.5) with different concentrations of salts. For each sample, the measurements were performed at room temperature from 200 to 320 nm with a scanning rate of 100 nm min^{-1} and each final spectrum was the average of three scans. The scans of the buffer alone containing the same concentration of salt were measured under the same experimental conditions and used as the background correction.

Sedimentation velocity experiments

Sedimentation velocity (SV) experiments were performed on a Proteomelab XL-A/I analytical ultracentrifuge (Beckman Coulter Instruments) with an An-60 Ti 4-hole rotor assembled by three cells and a counterbalance. UV-vis absorbance optics was used in this study to monitor the sedimentation and diffusion processes of DNA. Before each measurement, a volume of 400 μL of DNA solution with different concentrations of salts and a 410 μL of corresponding buffer without DNA as the reference were loaded into the cell assembled by a two-sector, charcoal-filled Epon centerpiece and two quartz windows. All experiments were conducted at 20.0 °C with a rotational speed of 58 000 rpm at a wavelength range of 260 to 300 nm. The criterion for selecting the appropriate wavelength is that the absorbance should be in the range of 0.5 and 1.0. About 250 scans for each cell were collected during each SV experiment and analyzed by SEDFIT using a continuous distribution $c(s)$ model which can separate the effects of diffusion and sedimentation of the solute.[55–57] In the SEDFIT software, the maximum entropy

regularization which follows the CONTIN method provided by Provencher[58,59] is used to solve the Lamm equation (eqn (1)).

$$\frac{\partial c}{\partial t} = \frac{1}{r}\frac{\partial}{\partial r}\left[r \cdot D\frac{\partial c}{\partial r} - \omega^2 r^2 sc\right] \quad (1)$$

where c, r, t, ω, s and D are the concentration of the solute, radial distance from the axis of rotation, sedimentation time, angular velocity, sedimentation coefficient and diffusion coefficient, respectively. With the combination of the Svedberg equation and the Stokes–Einstein equation:

$$M = \frac{s \cdot k_B \cdot N_A \cdot T}{D \cdot (1 - \bar{\nu} \cdot \rho_s)} \quad (2)$$

$$D = \frac{k_B \cdot T}{f} = \frac{k_B \cdot T}{6\pi\eta R_h} \quad (3)$$

we can obtain the information of molar mass M and hydrodynamic radius R_h, where the k_B, N_A, T, ρ_s, $\bar{\nu}$, f and η refer to the Boltzmann constant, Avogadro's number, absolute temperature, solvent density, partial specific volume of the solute, frictional coefficient, and solvent viscosity, respectively. Herein, we measured the value of the partial specific volume ($\bar{\nu}$) of DNA in different salt solutions by the density contrast sedimentation velocity according to Schuck *et al.*[60] The measured values of $\bar{\nu}$ are 0.55 ml g^{-1} for K/DNA, Na/DNA, Li/DNA and Tris/DNA and 0.47 ml g^{-1} for Cs/DNA when the concentration of CsCl is higher than 1.0 mM, which are similar to the earlier reports.[36,61–63] To eliminate the effect of different solvents on the sedimentation coefficient, the experimental sedimentation coefficient ($s_{20,exp}$) can be easily converted to the standard conditions ($s_{20,w}$) by means of eqn (4)[64]

$$s_{20,w} = s_{20,exp}\left(\frac{\eta_{20,s}}{\eta_{20,w}}\right)\left(\frac{1 - \bar{\nu}\rho_{20,w}}{1 - \bar{\nu}\rho_{20,s}}\right) \quad (4)$$

where $s_{20,exp}$ and $s_{20,w}$ are the experimental sedimentation coefficient and the standard sedimentation coefficient in water at 20.0 °C, respectively. $\eta_{20,s}$, $\eta_{20,w}$, $\rho_{20,s}$ and $\rho_{20,w}$ are the viscosity and density of solvent and water at 20.0 °C, respectively.

Results and discussion

The effect of potassium ions on the conformation of HT-DNA

Both nuclear magnetic resonance (NMR) and laser light scattering (LLS) can be used to determine the structural and hydrodynamic properties of DNA, while the concentration needed in these experiments is relatively high. DNA chains may form dimers, trimers and multimers at high concentrations, and thus it is difficult to study a single-molecule behavior with these two techniques.[9,32] Moreover, the fluorescence method can be used to study the single molecular behavior because of its high sensitivity, however, the labeling with extrinsic fluorophores or the substitutions of 2-aminopurine for adenine bases might influence the structural properties of DNA.[22,27,65] In this study, we use analytical ultracentrifugation (AUC) to study the hydrodynamic properties of human telomere DNA (HT-DNA) in different salt solutions as AUC is a powerful technique to investigate the solution properties of biomacromolecules without labeling.[7,36–39,47–53,66–69] After loading sufficient data to SEDFIT (version 14.1),[55,66] we chose the continuous distribution $c(s)$ model with maximum entropy regularization to fit the data and the standard sedimentation coefficients ($s_{20,w}$), diffusion coefficients (D) and weight-average molecular weights (M_w) can be obtained. Fig. 1 shows typical standard sedimentation coefficient distributions of HT-DNA and control DNA in 10.0 mM Tris–HCl buffer solutions (pH = 7.5) with different concentrations of potassium ions (K^+), where the concentration of each DNA was kept at 2.0 μM. Each unimodal distribution of $s_{20,w}$ with a molecular weight (M_w) of about 7.0×10^3 g mol^{-1} indicates a single-molecule behavior. Moreover, both $s_{20,w}$ of control DNA and HT-DNA increase with the concentration of K^+, but the change in $s_{20,w}$ of HT-DNA is larger than that for control DNA because of the additional conformational change from a random coil to the G-quadruplex structure.

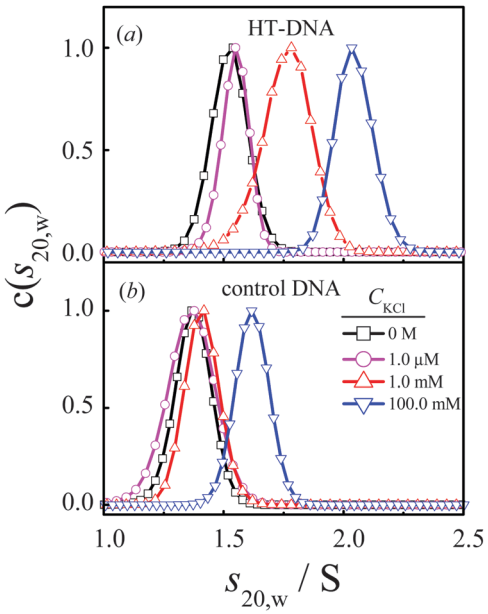

Fig. 1 Normalized sedimentation coefficient distribution of (a) HT-DNA and (b) control DNA at different concentrations of KCl, where the concentrations of HT-DNA and control DNA were 2.0 μM.

To determine the structural change of HT-DNA with the increasing concentration of KCl, the CD spectra of HT-DNA with different concentrations of KCl were measured, as shown in Fig. 2. We increased the concentration of HT-DNA to 8.0 μM to obtain a good signal-to-noise ratio in CD measurements. Note that there is no change in the standard sedimentation coefficient induced by KCl at two concentrations of DNA (2.0 μM and 8.0 μM), as shown in the ESI† (Fig. S1). Fig. 2 shows that a strong positive peak near 290 nm with a shoulder peak around 270 nm and a smaller negative peak around 235 nm are observed with the increasing concentration of K^+, indicating the formation of a hybrid-type G-quadruplex, which is consistent with earlier reports.[7,9,70,71] For control DNA, the CD spectra do not change with the increasing concentration of K^+, indicating no conformational change, as shown in the ESI† (Fig. S2).

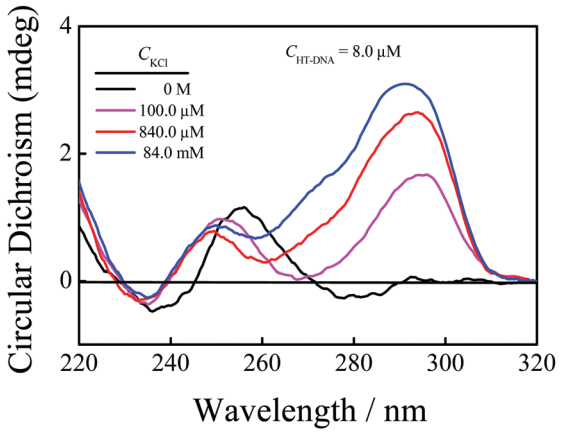

Fig. 2 CD spectra of the K^+-induced G-quadruplex of HT-DNA in a buffer solution (10.0 mM Tris–HCl, pH = 7.5) at 25 °C, where the concentration of HT-DNA was 8.0 μM.

Fig. 3(a) shows the influence of the K^+ concentration ranging from 0 to 1.0 M on the structural change of HT-DNA in detail. As a control, the standard sedimentation coefficient of a random sequenced-DNA in the presence of different concentrations of KCl was also measured. We can divide the whole region into three subregions, respectively. In subregion I, there is no change in $s_{20,w}$ of both HT-DNA and control DNA with the increase in C_{K^+}. $s_{20,w}$ of HT-DNA increases with C_{K^+} in subregion II. $s_{20,w}$ of control DNA only starts to increase in subregion III when the C_{K^+} is higher than 1.0 mM. It is known that polynucleotides as polyions exhibit polyelectrolyte properties in aqueous solutions in the presence of salts, so the counterions will condense onto the DNA chains to decrease the electrostatic repulsive interactions between phosphate groups of polynucleotides.[72,73] Moreover, the increase in the amount of the counterions can lead to an increase in the degree of adsorption of counterions and thus a decrease in the size of the polyions.[74–76] Nevertheless, there is no increase in $s_{20,w}$ of control DNA until the concentration of K^+ is above 1.0 mM, as shown in Fig. 3(a). Similarly, Sauer *et al.* reported that the addition of NaCl has no effect on the counterion condensation of a poly(T) when the NaCl concentration is smaller than 1 mM as the solution contains 10 mM sodium phosphate.[77] Thus a small amount of K^+ less than 1.0 mM added into the system containing 10.0 mM Tris has no obvious effect on the counterion condensation and the standard sedimentation coefficient of control DNA. However, $s_{20,w}$ of HT-DNA starts to increase with C_{K^+} when C_{K^+} is higher than 10.0 μM which is much smaller than 1.0 mM. For HT-DNA, besides the non-specific electrostatic interaction which weakens the electrostatic repulsion between nucleotides, specific interactions between the dehydrated cations and O6 of guanine also exist.[2,9] The specific interactions stabilize the G-tetrad formed by four guanines and promote the formation of the intra-molecular G-quadruplex accompanying an increase in $s_{20,w}$ with a small K^+ concentration of ~10.0 μM, which was also verified by CD experiments.

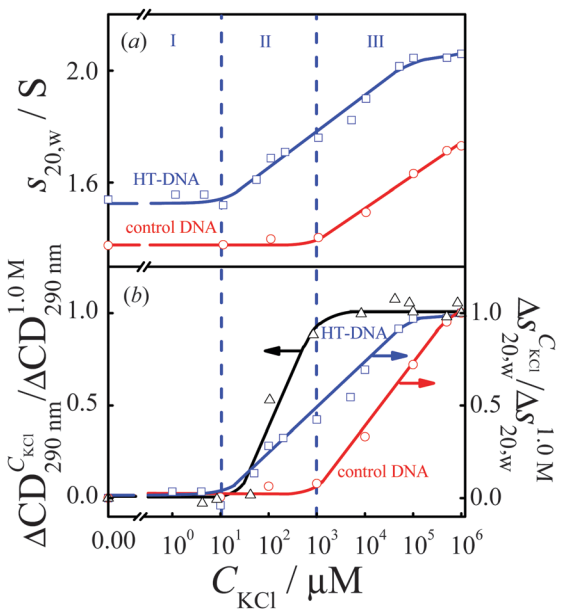

Fig. 3 (a) KCl concentration dependence of the standard sedimentation coefficient of HT-DNA and control DNA. (b) Normalized CD signal and standard sedimentation coefficient as a function of KCl concentration, where $\Delta CD^{C_{KCl}}_{290nm} = CD^{C_{KCl}}_{290nm} - CD^{0M}_{290nm}$, $\Delta CD^{1.0M}_{290nm} = CD^{1.0M}_{290nm} - CD^{0M}_{290nm}$, $\Delta s^{C_{KCl}}_{20,w} = s^{C_{KCl}}_{20,w} - s^{0M}_{20,w}$ and $\Delta s^{1.0M}_{20,w} = s^{1.0M}_{20,w} - s^{0M}_{20,w}$.

To visually distinguish the different contributions of specific and non-specific interactions to $s_{20,w}$ of HT-DNA, Fig. 3(b) shows the normalized signals of CD and $s_{20,w}$. With the increase in K^+ concentration the CD signal of HT-DNA increases and levels off when the concentration of K^+ is larger than 1.0 mM, indicating that the folding process is complete, which is similar to the results reported by Chaires *et al.*[46] Thus, the increase in $s_{20,w}$ of HT-DNA in the subregion II is due to the formation of the G-quadruplex. In the subregion III, the increase in $s_{20,w}$ of HT-DNA and control DNA is presumably due to the non-specific interactions between phosphate groups and K^+, which make the sedimentation of DNA much faster.

The effects of specific cations on the formation of the G-quadruplex

Fig. 4 shows the standard sedimentation coefficient distributions of HT-DNA in 100.0 mM LiCl, NaCl, KCl and CsCl solutions. The unimodal distribution indicates a unimolecular behavior of HT-DNA upon addition of these salts. A significant difference in $s_{20,w}$ in the presence of different salts is observed, which will be discussed as follows. First of all, from the Svedberg equation, we know that the sedimentation coefficient of macromolecules is proportional to buoyant mass [$M_b = M(1 - \bar{\nu}\rho_s)$] divided by the hydrodynamic radius of the macromolecules. Note that the influence of the density and viscosity of the solvent is eliminated by the use of the standard sedimentation coefficient. By fitting the sedimentation data to the continuous distribution $c(s)$ model with SEDFIT, we can obtain the values of M_w and R_h with the relative standard errors less than 5%.[78] Since the molecular weight of cations decreases in the order $Cs^+ > K^+ > Na^+ > Li^+$, M_w of HT-DNA decreases in the order $M_{w,CsCl}$ (8.0×10^3 g mol^{-1}) > $M_{w,KCl}$ (6.9×10^3 g mol^{-1}) ≈ $M_{w,NaCl}$ (7.0×10^3 g mol^{-1}) ≈ $M_{w,LiCl}$ (6.7×10^3 g mol^{-1}). As reported by

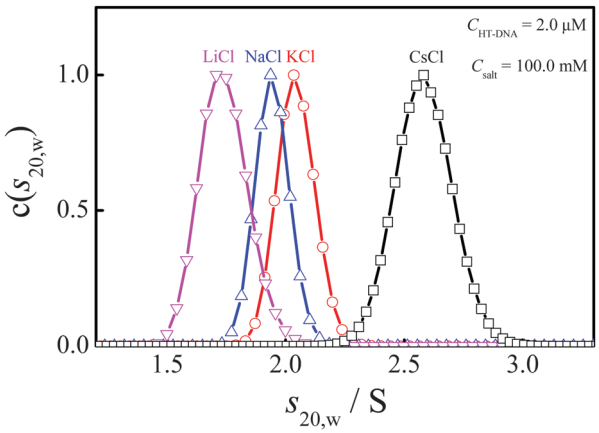

Fig. 4 Normalized standard sedimentation coefficient ($s_{20,w}$) distributions of HT-DNA in different salt aqueous solutions, where the concentrations of HT-DNA and each salt were 2.0 μM and 100.0 mM, respectively.

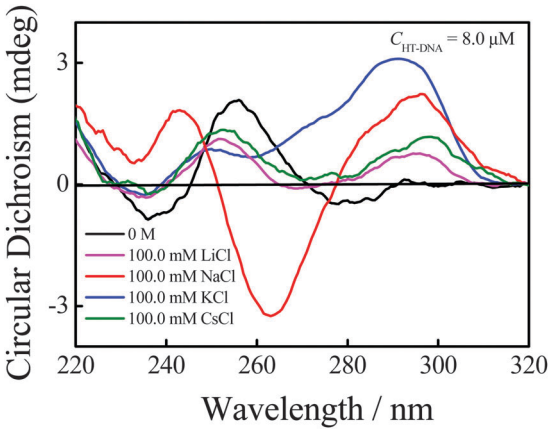

Fig. 5 CD spectra of the cation-induced G-quadruplex folding in the presence of different cations in a buffer solution (10.0 mM Tris/HCl, pH = 7.5) at 25 °C, where the concentration of HT-DNA was 8.0 μM.

Hearst *et al.*, the density of Cs/DNA (2.09 g ml^{-1}) is higher than the density of K/DNA (1.78 g ml^{-1}), Na/DNA (1.80 g ml^{-1}) and Li/DNA (1.78 g ml^{-1}).[61] Thus, $M_{b,CsCl} > M_{b,KCl} \approx M_{b,NaCl} \approx M_{b,LiCl}$. Moreover, the hydrodynamic radius of HT-DNA in each salt solution obeys the order $R_{h,LiCl}$ (1.52 nm) = $R_{h,CsCl}$ (1.52 nm) > $R_{h,NaCl}$ (1.43 nm) > $R_{h,KCl}$ (1.34 nm). Second, the so-called secondary salt effect, which refers to a new electric field created by the salt ions due to the different sedimentation rates of various ions, should also be considered, where the secondary salt effect obeys the order CsCl > KCl > NaCl > LiCl.[79] Thus, with the combination of these effects mentioned above, we have $s_{CsCl} > s_{KCl} > s_{NaCl} > s_{LiCl}$ with the same salt concentration of 100.0 mM.

The CD spectra of HT-DNA in 100.0 mM LiCl, NaCl, KCl and CsCl solutions were also measured, as shown in Fig. 5. In contrast to the hybrid-type G-quadruplex formed in the presence of 100.0 mM K^+, as shown in Fig. 2, Fig. 5 shows a positive peak at 295 nm and a negative peak at 265 nm with the addition of 100.0 mM Na^+, which is characterized in a basket-stranded G-quadruplex according to the previous studies.[7,9] For Li^+ (or Cs^+), a positive peak located at 295 nm is also observed, while its signal is much weaker than that for Na^+ and K^+.

Furthermore, the structures of HT-DNA in different salt solutions with the concentration ranging from 0 to 1.0 M were measured by CD (the data are not shown). The intensity curves of CD signals at characteristic wavelengths (290 nm for the KCl solution and 295 nm for the other three salt solutions) are shown in Fig. 6. Without the addition of a salt, the CD signal of HT-DNA is around 0, indicating a random coil conformation.[32,70] The gradually increased signal with increasing salt concentration indicates the formation of the G-quadruplex. As discussed in Fig. 3(b), HT-DNA starts to fold with the addition of 10.0 μM KCl and the folding completes when the concentration of KCl increases to 1.0 mM. From Fig. 6, we can also see the folding process of HT-DNA in other three salt solutions. With the addition of NaCl, the CD signal starts to increase at 100.0 μM, and then the signal reaches its maximum and levels off with a further increase in salt concentration when the concentration of

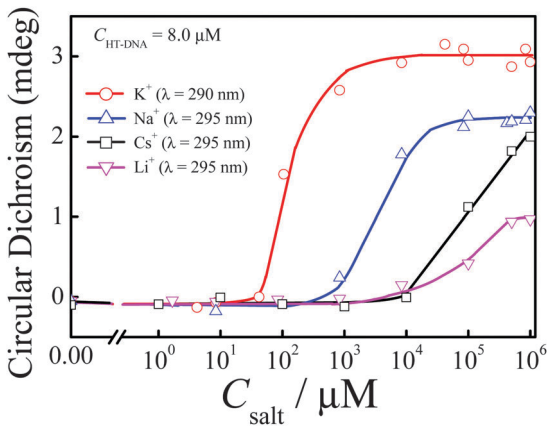

Fig. 6 Salt concentration dependence of the CD signal of HT-DNA in aqueous solutions, where the concentration of HT-DNA was 8.0 μM.

NaCl is higher than 20.0 mM, indicating a fully folded structure. Nevertheless, in the presence of LiCl or CsCl, the CD signal only starts to increase when the concentration is higher than 1.0 mM, where the non-specific interactions are dominant as we discussed before. The CD signal is still increasing when the concentration of Cs^+ or Li^+ is already above 100.0 mM, indicating that the folding of HT-DNA is not complete. The different concentrations of each type of cation needed for starting and complete folding of HT-DNA suggest the difference in the ability of these cations to induce the formation of the G-quadruplex.

Fig. 7 shows the salt concentration dependence of the standard sedimentation coefficient and the percentage increase in $s_{20,w}$ of HT-DNA (a) and control DNA (b). Fig. 7(b) shows $s_{20,w}$ of control DNA is nearly a constant when the concentration of each salt is smaller than 1.0 mM, and it starts to increase with different extents with further addition of salts. To visually investigate the change in $s_{20,w}$ of HT-DNA (or control DNA) with the addition of salt, we show the percentage increase in $s_{20,w}$ (f%) at the right side of the Y axis, where $f = (s_{20,w} - s_{20,w,0})/s_{20,w,0} \times 100$.

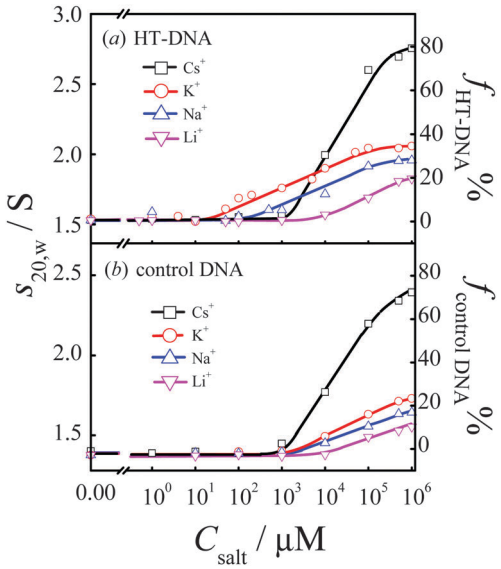

Fig. 7 Salt concentration dependence of the standard sedimentation coefficient and the percentage increase in $s_{20,w}$ (f%) of (a) HT-DNA and (b) control DNA in aqueous solutions, where the concentration of each DNA was 2.0 μM. f% is defined as $(s_{20,w} - s_{20,w,0})/s_{20,w,0} \times 100$ and $s_{20,w,0}$ refers to $s_{20,w}$ of HT-DNA (or control DNA) in the buffer solutions without the addition of these four types of salts.

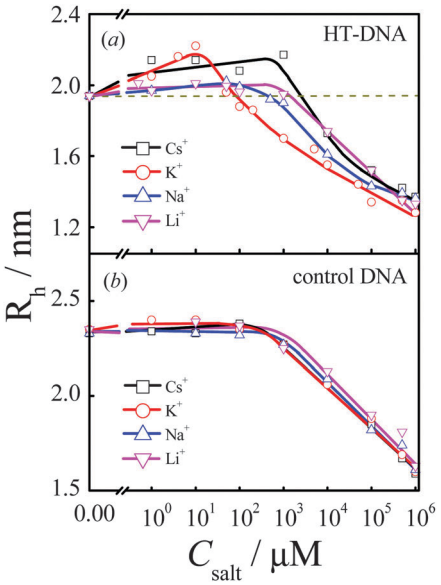

Fig. 8 Salt concentration dependence of the hydrodynamic radius of (a) HT-DNA and (b) control DNA in aqueous solutions, where the concentration of each DNA was 2.0 μM.

With the addition of 100.0 mM Cs^+, K^+, Na^+ and Li^+, the change in $s_{20,w}$ for control DNA is 56.8%, 16.4%, 13.1% and 6.3%, respectively, which is due to the non-specific counterion condensation by noting that there is no specific interactions between control DNA and salts. The different changes in $s_{20,w}$ may be due to the different changes in buoyant mass M_b and the second salt effect, as mentioned in Fig. 4. For HT-DNA, the minimum concentration of cations required to induce the increase in $s_{20,w}$ follows the order K^+ (~10.0 μM) < Na^+ (~100.0 μM) < Cs^+ ≈ Li^+ (~1.0 mM), *i.e.* the ability of cation-induced formation of the G-quadruplex follows the order $K^+ > Na^+ > Cs^+ \approx Li^+$, which is consistent with the CD results shown in Fig. 6. Previous reports also showed that the ability of cations to induce the formation of the G-quadruplex is different.[41,80,81] By the use of an ultrafast microfluidic mixer, Liu *et al.* showed that the folding rate of the G-quadruplex formed from $(d(TTAGGG)_4)$ was more rapid in K^+ solution than that in Na^+ solution.[40] The dehydrated K^+ ion is more suitable for the G-quartet than Na^+, not only because of a better fit size of dehydrated K^+, but also due to the lower energetic cost of dehydration of K^+. Note that it was reported that the dehydrated radius of ions obeys the order $Li^+ < Na^+ < K^+ < Cs^+$.[82–85] The results obtained from large angle X-ray scattering (LAXS) and double difference infrared spectroscopy (DDIR) suggested that the smaller lithium ion is more strongly hydrated than Na^+, K^+ and then Cs^+.[86] Therefore, it is more difficult for Li^+ to dehydrate and then bind with the G-quadruplex due to its small size and high extent of hydration.[72,82] Furthermore, the size of dehydrated Cs^+ is too large to fit the cavity of the G-quartet. The main interactions between Li^+, Cs^+ and HT-DNA are non-specific interactions, which are responsible for the increase in $s_{20,w}$ when the concentration is higher than 1.0 mM, as shown in Fig. 7(a). The percentage increase in $s_{20,w}$ of HT-DNA in the presence of 100.0 mM Cs^+, K^+, Na^+ and Li^+ is 69.6%, 33.4%, 25.0% and 10.3%, respectively. The changes in $s_{20,w}$ for HT-DNA are more pronounced than that for control DNA, which resulted from the additional formation of the G-quadruplex.

The hydrodynamic radius (R_h) is a critical property to characterize the effect of cations on DNA. In SV experiments, we can obtain the values of D and R_h by fitting the sedimentation data with SEDFIT. Fig. 8 shows the changes in R_h of HT-DNA (a) and control DNA (b) with the increase in salt concentration. As shown in Fig. 8(b), a larger R_h value indicates that the control DNA with a small concentration of salts adopts a more extended conformation in the solutions. When the concentration of each salt reaches 1.0 mM, R_h decreases with the concentration of salt, which is due to the non-specific interactions. The salt concentration where the non-specific interactions start to work is in good agreement with the value obtained from Fig. 7(b). The salt-induced condensation of DNA is a common phenomenon in the aqueous solutions of polyions. Using fluorescence correlation spectroscopy (FCS), Sauer *et al.* studied the hydrodynamic properties of polythymine in the 10 mM sodium phosphate buffer solution, and they found that the hydrodynamic radius (R_h) remains unchanged when the NaCl concentration is smaller than 10 mM, and scales with concentration of added NaCl with an exponent $\alpha = (-0.11 \pm 0.01)$ when the NaCl concentration is higher than 10 mM.[77] Here, R_h scales with the salt concentration as $R_h \propto C^\alpha$ with the exponents for these four types of cations between −0.043 and −0.051 and has a weak cation-dependence. Note that the difference between the values of the exponents in our study and the value (−0.11) reported by Sauer *et al.* may be due to the different lengths and sequences of DNA samples and/or the species of buffers.

Fig. 8(a) shows that the trends of R_h with the increasing concentration of salt are different from that for control DNA. With the addition of cations, the R_h value of HT-DNA first slightly increases, which might reflect that there are some intermediate structures during the early folding process or the interaction between guanine and cations is different from the interactions between other nucleobases and cations by noting that there is no increase in R_h of control DNA at low cation concentration (1.0 μM–1.0 mM). Using the molecular dynamics simulations to study the interactions between cations and a double-stranded DNA, Shen *et al.* showed that K^+ and Cs^+ have a much stronger ability to coordinate to guanine.[87] Further addition of salts leads to a decrease in R_h, which is the result of the formation of the G-quadruplex and the decrease in the intramolecular electrostatic repulsion as discussed before, and the concentration required to induce a decrease in R_h of each cation obeys the order K^+ (~10.0 μM) < Na^+ (~100.0 μM) < $Cs^+ \approx Li^+$ (~1.0 mM). The difference in the critical concentration of these salts is due to the specific interactions, which has been mentioned in Fig. 7. Moreover, in contrast to control DNA, the value of R_h of HT-DNA has a significant cation-dependence. For example, as shown in Fig. 8(a), when the salt concentration reaches 100.0 mM, the value of HT-DNA in each salt solution obeys the order $R_{h,CsCl} \approx R_{h,LiCl} > R_{h,NaCl} > R_{h,KCl}$. Here, the different R_h may be due to the different conformations of HT-DNA exhibited in the different salt solutions, which are characterized by CD as shown in Fig. 5 and 6. And it was also reported that the G-quadruplex formed in the KCl solution is more compact than that in the NaCl solution,[7] which is in good agreement with our results. From Fig. 6, we know that HT-DNA is fully folded in the 100.0 mM NaCl and KCl solution while it is not fully folded in the presence of 100.0 mM LiCl and CsCl.

Fig. 9 shows the changes in the molecular weight of HT-DNA (a) and control DNA (b) determined by the Svedberg equation

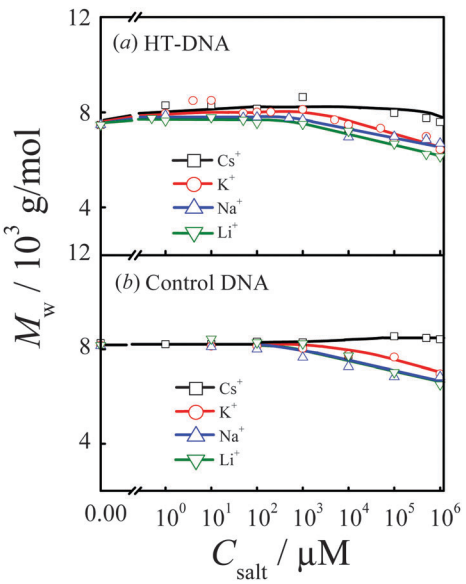

Fig. 9 Salt concentration dependence of M_w of (a) HT-DNA and (b) control DNA in aqueous solutions, where the concentration of each DNA was 2.0 μM.

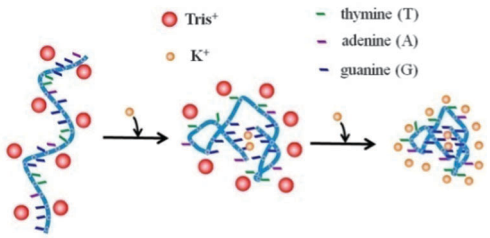

Fig. 10 Schematic diagram of the effects of K^+ on the conformation of HT-DNA.

(eqn (2)) with the increase in concentration of Cs^+, K^+, Na^+ and Li^+. In the buffer solution without any addition of salt, with $Tris^+$ as the counterion, the apparent molecular weight of HT-DNA and control DNA is 7.5 × 10^3 g mol^{-1} and 8.2 × 10^3 g mol^{-1}, respectively. For both DNA chains, there is a small change in molecular weight when the addition of salt concentration is smaller than 1.0 mM. While, when the concentrations of KCl, NaCl and LiCl are larger than 1.0 mM the counterions gradually change to K^+, Na^+ and Li^+, respectively. Hence, the apparent molecular weight of HT-DNA decreases accordingly, as shown in Fig. 9(a) and (b). With the increasing concentration of Cs^+ with a similar molecular weight of $Tris^+$, the molecular weights of HT-DNA and control DNA remain essentially unchanged. Furthermore, the M_w of HT-DNA over the whole salt concentration range is similar to the true molecular weight of monomeric HT-DNA, indicating an intramolecular conformational change and that there are no dimers and multimers in our system. Fig. 10 visually demonstrates the effects of K^+ on the conformation of HT-DNA.

Conclusions

The interactions between the G-quadruplex and cations in the system are very important to the structure of the G-quadruplex. By a combination of AUC and CD, we studied the effects of K^+ on the conformation of HT-DNA and control DNA. For control DNA, the minimum concentration of K^+ used to induce an increase in $s_{20,w}$ and a decrease in R_h is about 1.0 mM, which is due to the non-specific counterion condensation. 10.0 μM K^+ can induce an increase in $s_{20,w}$ and a decrease in R_h of HT-DNA due to the specific interactions. The results suggested that the specific interactions work prior to the non-specific interactions in our system containing 10.0 mM Tris. Moreover, the M_w of HT-DNA obtained from $s_{20,w}$ and R_h is similar to the true molecular weight of HT-DNA, suggesting an intra-molecular folding. Furthermore, the studies of the effects of the species of cations on the folding of HT-DNA show that the ability of cations to induce the formation of the G-quadruplex we studied obey the order $K^+ > Na^+ > Cs^+ \approx Li^+$.

Acknowledgements

The financial support of the National Program on Key Basic Research Project (2012CB933800), the National Natural Scientific Foundation of China (NNSFC) Projects (21274140) and the

Fundamental Research Funds for the Central Universities (WK2340000066) is gratefully acknowledged.

Notes and references

1 D. Sen and W. Gilbert, *Nature*, 1988, **334**, 364–366.
2 J. R. Williamson, M. K. Raghuraman and T. R. Cech, *Cell*, 1989, **59**, 871–880.
3 W. Guschlbauer, J. F. Chantot and D. Thiele, *J. Biomol. Struct. Dyn.*, 1990, **8**, 491–511.
4 Y. Wang and D. J. Patel, *Structure*, 1993, **1**, 263–282.
5 A. T. Phan and D. J. Patel, *J. Am. Chem. Soc.*, 2003, **125**, 15021–15027.
6 J. T. Davis, *Angew. Chem., Int. Ed.*, 2004, **43**, 668–698.
7 J. Li, J. J. Correia, L. Wang, J. O. Trent and J. B. Chaires, *Nucleic Acids Res.*, 2005, **33**, 4649–4659.
8 K. N. Luu, A. T. Phan, V. Kuryavyi, L. Lacroix and D. J. Patel, *J. Am. Chem. Soc.*, 2006, **128**, 9963–9970.
9 A. Ambrus, D. Chen, J. Dai, T. Bialis, R. A. Jones and D. Yang, *Nucleic Acids Res.*, 2006, **34**, 2723–2735.
10 M. C. Miller, R. Buscaglia, J. B. Chaires, A. N. Lane and J. O. Trent, *J. Am. Chem. Soc.*, 2010, **132**, 17105–17107.
11 S. Burge, G. N. Parkinson, P. Hazel, A. K. Todd and S. Neidle, *Nucleic Acids Res.*, 2006, **34**, 5402–5415.
12 E. H. Blackburn and J. W. Szostak, *Annu. Rev. Biochem.*, 1984, **53**, 163–194.
13 E. H. Blackburn, *Nature*, 1991, **350**, 569–573.
14 V. L. Makarov, Y. Hirose and J. P. Langmore, *Cell*, 1997, **88**, 657–666.
15 E. H. Blackburn, *Nature*, 2000, **408**, 53–56.
16 J. L. Mergny, J. F. Riou, P. Mailliet, M. P. Teulade-Fichou and E. Gilson, *Nucleic Acids Res.*, 2002, **30**, 839–865.
17 D. Y. Sun, B. Thompson, B. E. Cathers, M. Salazar, S. M. Kerwin, J. O. Trent, T. C. Jenkins, S. Neidle and L. H. Hurley, *J. Med. Chem.*, 1997, **40**, 2113–2116.
18 S. Neidle and G. Parkinson, *Nat. Rev. Drug Discovery*, 2002, **1**, 383–393.
19 I. Bessi, H. R. A. Jonker, C. Richter and H. Schwalbe, *Angew. Chem., Int. Ed.*, 2015, **54**, 8444–8448.
20 K. Phillips, Z. Dauter, A. I. H. Murchie, D. M. J. Lilley and B. Luisi, *J. Mol. Biol.*, 1997, **273**, 171–182.
21 P. Hazel, J. Huppert, S. Balasubramanian and S. Neidle, *J. Am. Chem. Soc.*, 2004, **126**, 16405–16415.
22 C. S. Mekmaysy, L. Petraccone, N. C. Garbett, P. A. Ragazzon, J. O. Trent and J. B. Chaires, *J. Am. Chem. Soc.*, 2008, **130**, 6710–6711.
23 H. Zhu, S. Y. Xiao and H. J. Liang, *PLoS One*, 2013, **8**, e71380.
24 R. M. Abu-Ghazalah, S. Rutledge, L. W. Lau, D. N. Dubins, R. B. Macgregor, Jr. and A. S. Helmy, *Biochemistry*, 2012, **51**, 7357–7366.
25 B. G. Kim, Y. L. Shek and T. V. Chalikian, *Biophys. Chem.*, 2013, **184**, 95–100.
26 J. Mohanty, N. Barooah, V. Dhamodharan, S. Harikrishna, P. I. Pradeepkumar and A. C. Bhasikuttan, *J. Am. Chem. Soc.*, 2013, **135**, 367–376.
27 L. Ying, J. J. Green, H. Li, D. Klenerman and S. Balasubramanian, *Proc. Natl. Acad. Sci. U. S. A.*, 2003, **100**, 14629–14634.
28 M. Bončina, J. Lah, I. Prislan and G. Vesnaver, *J. Am. Chem. Soc.*, 2012, **134**, 9657–9663.
29 B. Pagano, A. Randazzo, I. Fotticchia, E. Novellino, L. Petraccone and C. Giancola, *Methods*, 2013, **64**, 43–51.
30 A. Marchand, R. Ferreira, H. Tateishi-Karimata, D. Miyoshi, N. Sugimoto and V. Gabelica, *J. Phys. Chem. B*, 2013, **117**, 12391–12401.
31 A. Marchand, A. Granzhan, K. Iida, Y. Tsushima, Y. Ma, K. Nagasawa, M. Teulade-Fichou and V. Gabelica, *J. Am. Chem. Soc.*, 2015, **137**, 750–756.
32 A. Wlodarczyk, P. Grzybowski, A. Patkowski and A. Dobek, *J. Phys. Chem. B*, 2005, **109**, 3594–3605.
33 Z. Y. Kan, Y. Lin, F. Wang, X. Y. Zhuang, Y. Zhao, D. W. Pang, Y. H. Hao and Z. Tan, *Nucleic Acids Res.*, 2007, **35**, 3646–3653.
34 Y. Amemiya, Y. Furunaga, K. Iida, M. Tera, K. Nagasawa, K. Ikebukuroa and C. Nakamura, *Chem. Commun.*, 2011, **47**, 7485–7487.
35 H. Wang, G. J. Nora, H. Ghodke and P. L. Opresko, *J. Biol. Chem.*, 2011, **286**, 7479–7489.
36 L. M. Hellman, D. W. Rodgers and M. G. Fried, *Eur. Biophys. J.*, 2010, **39**, 389–396.
37 N. C. Garbett, C. S. Mekmaysy and J. B. Chaires, *Methods Mol. Biol.*, 2010, **608**, 97–120.
38 L. Petraccone, C. Spink, J. O. Trent, N. C. Garbett, C. S. Mekmaysy, C. Giancola and J. B. Chaires, *J. Am. Chem. Soc.*, 2011, **133**, 20951–20961.
39 H. T. Le, W. L. Dean, R. Buscaglia, J. B. Chaires and J. O. Trent, *J. Phys. Chem. B*, 2014, **118**, 5390–5405.
40 Y. Li, C. Liu, X. Feng, Y. Xu and B. F. Liu, *Anal. Chem.*, 2014, **86**, 4333–4339.
41 R. D. Gray and J. B. Chaires, *Nucleic Acids Res.*, 2008, **36**, 4191–4203.
42 V. Kumar, A. Sengupta, K. Gavvala, R. K. Koninti and P. Hazra, *J. Phys. Chem. B*, 2014, **118**, 11090–11099.
43 N. V. Hud, F. W. Smith, F. A. L. Anet and J. Feigon, *Biochemistry*, 1996, **35**, 15383–15390.
44 H. K. Frensdorf, *J. Am. Chem. Soc.*, 1971, **93**, 600–606.
45 W. Xu, Q. G. Tan, M. Yu, Q. Sun, H. H. Kong, E. Laesgaard, I. Stensgaard, J. Kjems, J. G. Wang, C. Wang and F. Besenbacher, *Chem. Commun.*, 2013, **49**, 7210–7212.
46 R. D. Gray and J. B. Chaires, *Biophys. Chem.*, 2011, **159**, 205–209.
47 S. Wu, X. Y. Wang, X. D. Ye and G. Z. Zhang, *J. Phys. Chem. B*, 2013, **117**, 11541–11547.
48 M. Trajkovski, M. W. da Silva and J. Plavec, *J. Am. Chem. Soc.*, 2012, **134**, 4132–4141.
49 U. Dornberger, J. Behlke, E. BirchHirschfeld and H. Fritzsche, *Nucleic Acids Res.*, 1997, **25**, 822–829.
50 T. Laue, *Curr. Opin. Struct. Biol.*, 2001, **11**, 579–583.
51 M. C. Miller, H. T. Le, W. L. Dean, P. A. Holt, J. B. Chaires and J. O. Trent, *Org. Biomol. Chem.*, 2011, **9**, 7633–7637.
52 H. T. Le, M. C. Miller, R. Buscaglia, W. L. Dean, P. A. Holt, J. B. Chaires and J. O. Trent, *Org. Biomol. Chem.*, 2012, **10**, 9393–9404.
53 C. Rehm, I. T. Holder, A. Groß, F. Wojciechowski, M. Urban, M. Sinn, M. Drescher and J. S. Hartig, *Chem. Sci.*, 2014, **5**, 2809–2818.

54 H. T. Le, R. Buscaglia, W. L. Dean, J. B. Chaires and J. O. Trent, *Top. Curr. Chem.*, 2013, **330**, 179–210.
55 P. Schuck, *Biophys. J.*, 2000, **78**, 1606–1619.
56 J. Dam and P. Schuck, *Numerical Computer Methods, Pt E*, 2004, **384**, 185–212.
57 P. H. Brown and P. Schuck, *Biophys. J.*, 2006, **90**, 4651–4661.
58 S. W. Provencher, *Comput. Phys. Commun.*, 1982, **27**, 213–227.
59 S. W. Provencher, *Comput. Phys. Commun.*, 1982, **27**, 229–242.
60 P. H. Brown, A. Balbo, H. Y. Zhao, C. Ebel and P. Schuck, *PLoS One*, 2011, **6**, e26221.
61 J. E. Hearst, *J. Mol. Biol.*, 1962, **4**, 415–417.
62 R. B. J. Vinogard, *Biochim. Biophys. Acta*, 1965, **108**, 18–29.
63 G. Cohen and H. Eisenber, *Biopolymers*, 1968, **6**, 1077–1100.
64 W. Mächtle and L. Börger, *Analytical Ultracentrifugation of polymers and Nanoparticles*, Springer, Berlin, 2006.
65 P. Alberti and J. L. Mergny, *Proc. Natl. Acad. Sci. U. S. A.*, 2003, **100**, 1569–1573.
66 J. Lebowitz, M. S. Lewis and P. Schuck, *Protein Sci.*, 2002, **11**, 2067–2079.
67 C. Ebel, *Methods*, 2011, **54**, 56–66.
68 R. Buscaglia, M. C. Miller, W. L. Dean, R. D. Gray, A. N. Lane, J. O. Trent and J. B. Chaires, *Nucleic Acids Res.*, 2013, **41**, 7934–7946.
69 H. Y. Zhao, R. Ghirlando, C. Alfonso, F. Arisaka, I. Attali and D. L. Bain, *et al.*, *PLoS One*, 2015, **10**, e0126420.
70 M. Vorlickova, J. Chladkova, I. Kejnovska, M. Fialova and J. Kypr, *Nucleic Acids Res.*, 2005, **33**, 5851–5860.
71 Y. Xu, Y. Noguchi and H. Sugiyama, *Bioorg. Med. Chem.*, 2006, **14**, 5584–5591.
72 G. S. Manning, *Q. Rev. Biophys.*, 1978, **11**, 179–246.
73 M. D. N. Ngavouka, A. Bosco, L. Casalis and P. Parisse, *Macromolecules*, 2014, **47**, 8748–8753.
74 M. Balastre, F. Li, P. Schorr, J. C. Yang, J. W. Mays and M. V. Tirrell, *Macromolecules*, 2002, **35**, 9480–9486.
75 M. Muthukumar, *J. Chem. Phys.*, 2004, **120**, 9343–9350.
76 D. Bracha, E. Karzbrun, G. Shemer, P. A. Pincus and R. H. Bar-Ziv, *Proc. Natl. Acad. Sci. U. S. A.*, 2013, **110**, 4534–4538.
77 S. Doose, H. Barsch and M. Sauer, *Biophys. J.*, 2007, **93**, 1224–1234.
78 J. L. Cole, J. W. Lary, T. P. Moody and T. M. Laue, *Methods Cell Biol.*, 2008, **84**, 143–179.
79 K. O. Pedersen, *J. Phys. Chem.*, 1958, **62**, 1282–1290.
80 S. Takenaka and B. Juskowiak, *Anal. Sci.*, 2011, **27**, 1167–1172.
81 C. C. Hardin, T. Watson, M. Corregan and C. Bailey, *Biochemistry*, 1992, **31**, 833–841.
82 J. Kiella, *J. Am. Chem. Soc.*, 1973, **59**, 1675–1678.
83 J. N. Israelachvili, *Intermolecular and Surface Forces*, Elsevier, London, 3rd edn, 2011.
84 E. Largy, A. Marchand, S. Amrane, V. Gabelica and J. L. Mergny, *J. Am. Chem. Soc.*, 2016, **138**, 2780–2792.
85 Y. Kim, T.-T. T. Nguyen and D. G. Churchill, *Met. Ions Life Sci.*, 2016, **16**, 1–10.
86 J. Mahler and I. Persson, *Inorg. Chem.*, 2012, **51**, 425–438.
87 X. Shen, B. Gu, S. A. Che and F. S. Zhang, *J. Chem. Phys.*, 2011, **135**, 034509.